

High pressure bulk synthesis of InN by solid state reaction of binary oxide in a multi-anvil apparatus

Elena Del Canale,^{1,2} Lorenzo Fornari,^{1,2} Chiara Coppi,^{1,2} Giulia Spaggiari,^{1,3} Francesco Mezzadri,^{2,1} Giovanna Trevisi,¹ Patrizia Ferro,¹ Edmondo Gilioli,¹ Massimo Mazzer,¹ Davide Delmonte.¹*

¹ CNR – IMEM, 43124, Parma, Italy

² SCVSA Department, Università degli Studi di Parma, 43124, Parma, Italy

³ Department of Mathematical, Physical and Computer Sciences, Università degli Studi di Parma, 43124, Parma, Italy

*Corresponding Author: elena.delcanale@imem.cnr.it

KEYWORDS indium nitride, mechanochemistry, high pressure/high temperature synthesis

Abstract

We present a new method to synthesize bulk indium nitride by means of a simple solid-state chemical reaction carried out under hydrostatic high pressure/high temperature conditions in a multi-anvil apparatus, not involving gases or solvents during the process. The reaction occurs between the binary oxide In_2O_3 and the highly reactive Li_3N as nitrogen source, in powder form. The formation of the hexagonal phase of InN, occurring at 350 °C and $P \geq 3$ GPa, was successfully confirmed by powder X-ray diffraction, with the presence of Li_2O as unique byproduct. A simple

washing process in weak acidic solution followed by centrifugation, allowed to obtain pure InN polycrystalline powders as precipitate. With an analogous procedure it was possible to obtain pure bulk GaN, from Ga₂O₃ and Li₃N at $T \geq 600^\circ\text{C}$ and $P \geq 2.5$ GPa. These results point out, particularly for InN, a clean, and innovative way to produce significant quantities of one of the most promising nitrides in the field of electronics and energy technologies.

1. Introduction

Indium nitride, as well as its isostructural compound gallium nitride and their solid solutions, is a direct band gap III-V semiconductor of great interest in the field of electronics,^{1,2,3} high power devices^{4,5,6} and LED technologies,^{7,8} for its unique optical absorption properties. From the structural point of view, InN crystallizes in a wurtzite-like hexagonal cell (space group $P6_3mc$) characterized by lattice parameters $a = 3.536 \text{ \AA}$ and $c = 5.709 \text{ \AA}$.⁹ This black, low band-gap semiconductor ($E_g = 0.7 \text{ eV}$)¹⁰ shows a notable RT-conductivity, high absorption coefficient, very high thermal conductivity despite an intrinsic chemical instability due to the very weak In-N covalent bond.

InN electro-optical properties completely differ from those of its related compound, GaN, which is instead a white high band-gap semiconductor ($E_g = 3.4 \text{ eV}$)¹¹, looking yellowish due to the presence of defects. Even though isostructural, hexagonal GaN possesses a far smaller unit cell¹² due to the large difference (exceeding 30%) between the two cation ionic radii. As a consequence, GaN is characterized by complementary physical properties i.e., low RT-conductivity, low absorption coefficient and low thermal conductivity.

Due to these opposite characteristics, the stabilization of (In,Ga)N solid solutions, which in principle may allow to access an enormous range electro-optical/thermal properties and get into a wide gamma of technologies, results to be complex, limited at the nanoscale^{13,14,15,16,17,18,19,20,21,22} and far from application yet. Consequently, (In,Ga)N production still represents one of the biggest challenges for the scientific community working on this class of nitrides. At the origin of this

problem, there is basically the different stability of GaN and InN phases. Indeed, several successful examples of GaN synthesis have been reported in literature, both as film by hetero/homo-epitaxial growth methods (mainly with CVD,^{23,24} MOCVD,^{25,26,27,28} MBE,^{29,30,31,32} MOVPE^{33,34,35} and VPE³⁶) and as bulk by various crystal growth routes (such as high pressure/high temperature fluid-mediated synthesis methods, e.g. ammonothermal method,³⁷ high-pressure nitrogen solution growth process^{38,39} and Na-flux method under high pressure of the reactive atmosphere⁴⁰) and also via solid state high pressure/high temperature reaction exploiting a cubic anvil cell.^{41,42}

Vice versa there are only few reports of effective InN syntheses. This depends on the fact that InN has a low dissociation temperature (450°C⁴³), which makes the epitaxial growth at standard temperatures very difficult. Moreover, the synthesis of bulk crystalline InN results even more complex and tricky due to high instability of the In-N bond. In the case of profitable attempts, the reactions often occur under harsh conditions, through the use of toxic, polluting and very hazardous reactants, such as: ammonothermal growth from InCl₃ and KNH₂ in supercritical ammonia at 2.8 kbar,⁴⁴ solvothermal reaction of InCl₃/InI₃ with LiNH₂ in benzene,⁴⁵ microwave plasma sources at sub-atmospheric pressure by saturating indium with nitrogen,⁴⁶ low-temperature synthesis via nitridation of LiInO₂⁴⁷ or In(OH)₃⁴⁸ with NaNH₂ flux in autoclave, nitridation of In₂O₃ and In(OH)₃ with NH₃ at 600 °C,⁴⁹ solid-state exchange reaction between Ga/InI₃ and Li₃N⁵⁰ or InBr₃ and NaN₃.⁵¹ Despite the different methods and conditions, the reactions have a very low yield, somehow producing well shaped μm-scale crystals, but rarely a pure bulk product. For these reasons, the use of InN is mainly confined at the lab scale for research purposes, and the known synthesis methods are currently characterized by very high production costs and difficult scalability.

However, some works in literature showed that it is possible to obtain several nitrides also with simpler, cheaper, and scalable techniques, as the case of the mechanochemical (MC) reactions exploited for CrN,⁵² Si₃N₄,⁵³ ZrN,⁵⁴ GaN,⁵⁵ TiN⁵⁶ and Fe₃N₄.⁵⁷ In conclusion, new approaches to

synthesize bulk InN are needed to push forward the interest in this class of nitrides and their solid solutions.

Therefore, we started to investigate the MC of InN by applying different ball milling conditions during the treatment. On the basis of this study, the gathered information drove us to identify a new approach for the synthesis of such nitrides, by the use of hydrostatic high pressure/high temperature (HP/HT) reactions performed in a multi-anvil press. To the best of our knowledge, some nitrides have already been studied by analogous HP/HT methods, as in the case of AlN,⁵⁸ SrN₂ and γ -P₃N₅,⁵⁹ Ge₃N₄⁶⁰ by multi-anvil, c-BC₂N,⁶¹ B₁₃N₂⁶² by toroid-type high pressure apparatus, MoN and MoN_{1-x},⁶³ c-Si₃N₄,⁶⁴ PtN⁶⁵ by diamond anvil cell and NaN₃⁶⁶ by Merrill-Bassett type pressure cell. However, the only attempts to synthesize InN in HP/HT conditions (i.e., in the giga-Pascal pressure range, exceeding the kbar regime typical of the solvothermal methods previously reported), again led to the formation of tiny crystals from the direct synthesis of metallic indium and compressed nitrogen at 2 GPa and 700°C,⁶⁷ but neither exploiting simple solid-state reaction nor applying pressure with solid media.

In this paper, we show that a solid-state reaction under isotropic HP/HT conditions leads to the formation of pure bulk InN, starting from indium binary oxide and non-toxic nitrogen-based compounds, without the use of any organic solvents or gases during the process. The relatively mild conditions enable to obtain a significant amount of material, with high yield. The same procedure was then successfully applied for the synthesis of pure bulk GaN, finding the stability condition for temperatures higher than InN.

2. Experimental Methods

The mechano-chemical reactions (MC) were performed using a Pulverisette 7 Classic Line high energy planetary ball mill (Fristch GmbH), with sealed ZrO₂ jars (volume: 45 ml) and spheres (diameter: 10 mm). In₂O₃ (ChemPur, 99.99%) and a super-stoichiometric content (i.e., +50% of

excess) of Li_3N (Alfa Aesar, 99.4%) were used as precursors and mixed under inert atmosphere. The reactions were carried out under a controlled inert atmosphere in dry conditions, thus without the use of an assisting liquid, inserting the ball mill apparatus in a glove box with slight N_2 overpressure, varying the combination of the main MC parameters: rotational speed (RPM), ball-to-powder mass ratio (BPR) and reaction time (TIME).

High pressure high temperature (HP/HT) syntheses were performed in isotropic conditions through a multi-anvil 6/8 Walker-type press apparatus (Rockland Inco Corps.). The reaction was carried out starting from a 600-700 mg homogeneous mixture of powders of In_2O_3 (ChemPur, 99.99%) with a super-stoichiometric content (i.e., +50% of excess) of Li_3N (Alfa Aesar, 99.4%) in an Au capsule. Once the target pressure (in the 2.5 – 6 GPa range) was reached with a ramp rate of about 30kPa/min, the temperature was increased of 50°C/min until the desired value (in the 350 – 900 °C range). After the synthesis, the temperature was quenched down to room temperature and the pressure slowly released overnight. The products, obtained in form of dense cylinders (about 5x5x5 mm), are ground in an agate mortar or cut in form of discs to be further characterized.

The phase analysis was performed through Powder X-Ray Diffraction (PXRD), using two different diffractometers in Bragg-Brentano geometry: (I) for qualitative analysis of the products, a Thermo-Electron X'Tra diffractometer equipped with a Thermo Electron solid state Si(Li) detector was used. This instrument utilizes $\text{Cu-K}\alpha$ wavelength ($\lambda=1.5406 \text{ \AA}$) and data were collected with 0.05° step and 3s of counting time; (II) For quantitative data collection we exploited a Rigaku Smartlab XE diffractometer with $\text{Cu K}\alpha$ wavelength. A Ni filter was used to suppress the $\text{K}\beta$ contribution. 5.0° soller slits were located both on the incident and diffracted beam and data were collected using a HyPix3000 detector operating in 1D mode.

The morphology and composition of the samples were investigated with a Zeiss Auriga Compact Field-Emission Scanning Electron Microscope (SEM) equipped with an Oxford Xplore 30 Energy Dispersive Spectroscopy (EDS) system. SEM images were acquired by using both 20 kV and 5 kV

acceleration voltages of the primary electron beam. EDS analyses were conducted by exciting the samples with a 20 kV accelerated electron beam.

Raman measurements were carried out using a micro-Raman spectrometer (Horiba LabRam HR Evolution Raman) equipped with a confocal Olympus microscope and 10x, 50x, ULWD50x, 100x objectives (spatial resolutions of approximately 1 μm). The Micro-Raman apparatus is completed by a He-Ne laser emitting at 632.8 nm, BraggRate Notch Filters, Silicon CCD + InGaAs Diode Array detectors, gratings 300-600-1800 lines/mm, and density filters. The spectrometer was calibrated using the standard silicon Raman peak at 520.6 cm^{-1} before each measurement. The spectra here reported were recorded using the 100x objective, for 30 s and 4 repetitions.

3. Results and Discussion

The solid-state chemical reaction is a nitridation synthesis of the binary In oxide by the use of Li_3N (in super-stoichiometric ratio, 50% excess in order to balance the eventual weighting error coming from conspicuous water absorbance during the alkali nitride precursor preparation), as reported in equation (1):



3.1. Mechanochemistry of InN

A mechanochemical process exploits the non-equilibrium thermodynamics and very high local temperatures differently from conventional synthesis methods, accessible via high energy ball milling experiments. The application of this technique led, in the current case, to a better understanding of the InN formation process and the energy needed to initiate and complete the solid state nitridation reactions of equation (1), even though the MC regimes explored in this work did not allow to obtain InN.

In this study, we investigate a wide range of MC parameters exploring two complementary energy regimes, as comprehensively described in paragraph S.1 in the Supporting Information. It is

found that, for low MC energies ($400 < \text{RPM} \leq 600$), and independently from the ball-to-powder ratio and milling time, it is not possible to activate the nitridation reaction; the process indeed leads to a reduction of the mean crystallinity of the In_2O_3 phase (see **Figure S2** in the Supporting Information). Surprisingly, for high energies ($\text{RPM} > 600$), the lithium ions start to react with the oxygens of In_2O_3 ; however, the local mechanical energies are too high to metastabilize In-N bonds and consequently an unwanted redox process become favored: nitrogen ions oxidize, forming molecular gas by forcing In^{3+} reduction to metallic indium (**Figure 1** here below and **Figure S1** in the Supporting Information).

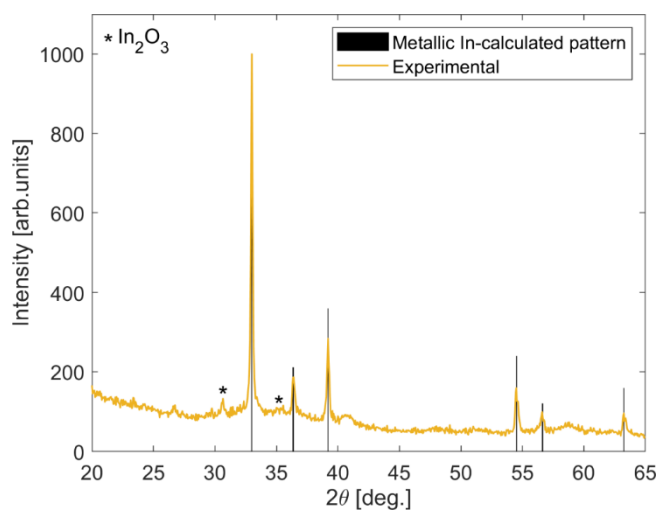


Figure 1. PXRD of the MC products obtained for the InN reaction by using 630RPM, 268 BPR and 40min of milling (yellow curve). The black vertical lines represent the calculated pattern of metallic In from ICSD using POWD-12++ 539, 3(1997), while the black “*” symbol represents the calculated In_2O_3 pattern from ICSD using POWD-12++1928, 1 (1997).

In brief, high energy ball milling processes seem to hinder the formation of InN so that the wanted reaction is quite inaccessible by MC, at least for an experiment conducted in N_2 atmosphere and dry conditions. These results suggest the use of a complementary approach for the study of this nitridation reaction. Therefore, a novel approach, consisting in the combination of high temperatures and high pressures through equilibrium thermodynamic solid-state reaction, is exploited to metastabilize the very weak In-N bond.

3.2. HP/HT InN syntheses

The same solid-state nitridation reaction was performed in the HP/HT regime, exploring different conditions of hydrostatic pressure (3 to 6 GPa), temperature (350 to 900°C) and duration (2 to 6 h), as summarized in **Table 1**. It was observed that the HP/HT synthesis of InN requires temperatures below 600 °C to prevent the formation of metallic In (**Figure S3**, blue curve in the Supporting Information) in close analogy to what observed with MC in high RPM regime. Particularly, the polycrystalline hexagonal InN was detected to form around 350 °C (yellow and purple curve **Figure S3**, in the Supporting Information).

PXRD analysis (**Figure S3** in the Supporting Information), highlights the systematical presence of ternary Li-based compounds, coming from a contamination of the highly hygroscopic Li₃N reactants (**Figure S8** in the Supporting Information), that can be almost completely removed with a washing treatment in acidic water but with a very low final mass yield of the InN product (**Figure S4** in the Supporting Information).

Table 1. InN explored HP/HT synthesis conditions.

Sample	Pressure [GPa]	Temperature [°C]	Time [h]	Nitride presence	Spurious In phases
InN	6	900	2	NO	YES
InN	3	750	2	NO	YES
InN	3.5	600	3	NO	YES
InN	6	390	6	YES	YES
InN	3	350	6	YES	YES
InN*	3.5*	350*	6*	YES	NO

* Reaction performed starting with new and pristine Li₃N reagents

The complete double exchange reaction (see equation (1)) is obtained through a HP/HT synthesis at 3.5 GPa, 350 °C and 1 h (**Figure 2**, upper panel), starting from a pristine Li_3N bottle. Noteworthy, besides InN, only Li_2O is present, as expected.

The sample powders are poured in acidic water (0.1M HCl) and then centrifuged at 4000 RPM for 15 min to separate InN from the other components, which are fully soluble in water. When Li_2O is put in water the solution pH rises, due to the formation of LiOH. To successfully remove all the amount of Li_2O the non-soluble suspension must be washed, centrifuged, and then separated from the aqueous solution several times, until neutral pH is reached. The precipitate is finally dried on a heating plate at 130 °C.

The PXRD results, reported in **Figure 2** (bottom panel), show the complete removal of the secondary phase, leaving a pure InN polycrystalline powder.

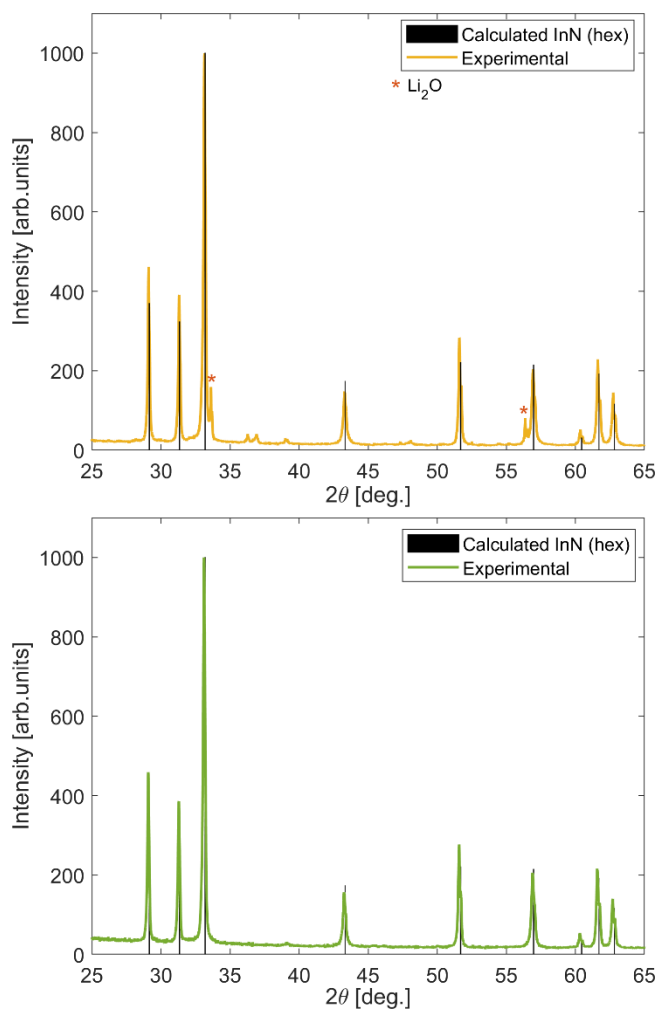


Figure 2. PXRD pattern collected for InN after the HP/HT synthesis (upper panel) and after the subsequent washing treatment (bottom panel), obtained at 3.5 GPa and 350°C. The black lines are the calculated reflections of the InN hexagonal phase calculated pattern from ICSD using POWD-12++ 46, 10086 (1997), while the orange “*” symbol correspond to the Li₂O phase, calculated from ICSD using POWD-12++40, 588 (1997).

SEM/EDX measurements (**Figure 3**) show that InN crystallites have sub-micrometrical dimensions around 100-200 nm, probably related to the reduced synthesis temperature, not allowing an effective sintering process. The effectiveness of the washing treatment in removing Li-based compounds from the HP/HT synthesized InN is confirmed by the compositional analysis: In and N are estimated with the expected ratio of 1:1, within the instrumental error. The C signal possibly comes from the carbon tape on which the powders are dispersed on the SEM probe, and the minor oxygen contribution could be ascribable to organic contamination on the surface.

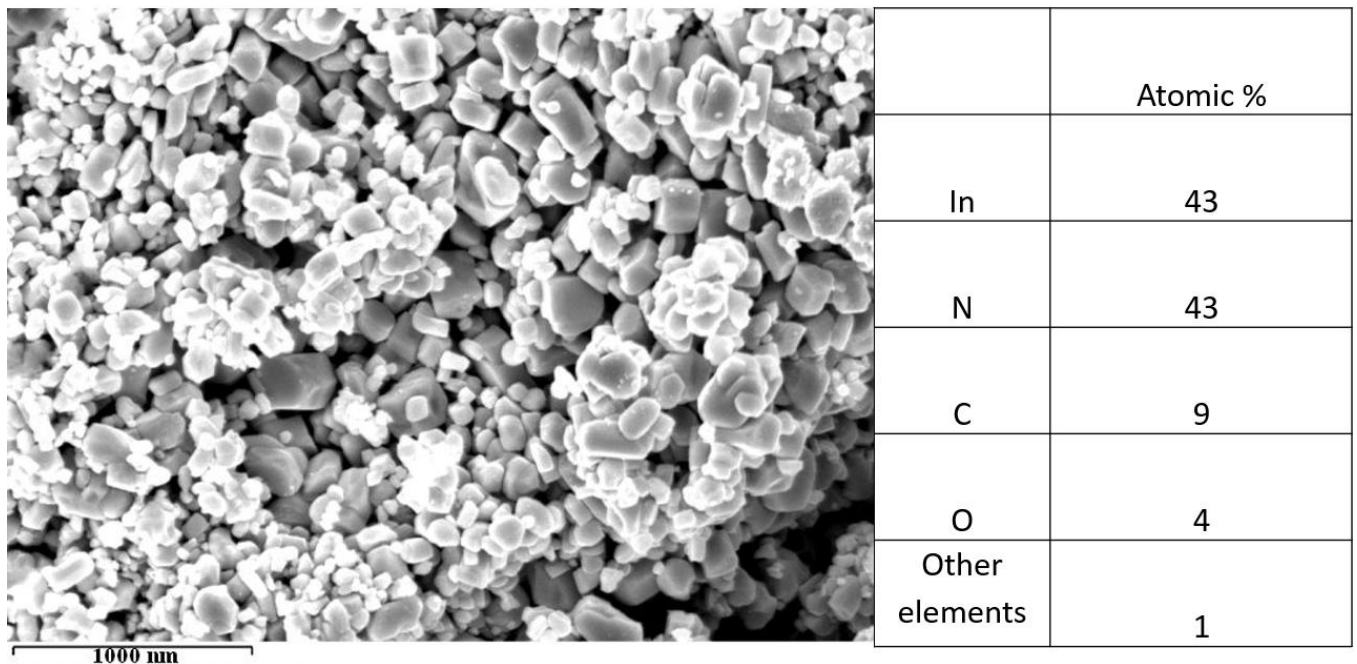


Figure 3. SEM image with 50kX magnification collected on hexagonal InN crystallites obtained at 350°C, 3 GPa, 1 h and relative atomic compositions.

The Raman spectra of InN (**Figure 4**) presents a noisy signal, ascribable to the observed relatively low crystallinity. However, the main peaks of the hexagonal phase⁶⁸ are still identifiable: 480 cm⁻¹ A₁ (TO), 476 cm⁻¹ E₁ (TO) and 580 cm⁻¹ A₁ (LO).

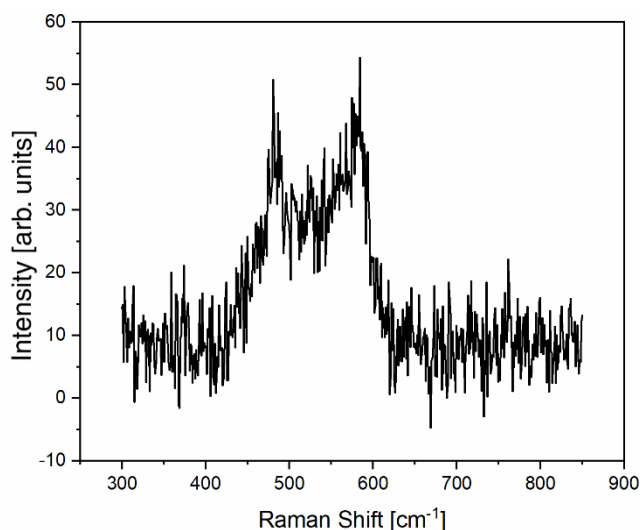


Figure 4. Raman spectra of InN powders after the washing treatment.

3.2.1 HP/HT synthesis of GaN

Analogous double-exchange reaction has been then studied for the synthesis of bulk GaN to find possible overlapping thermodynamic regimes in which both GaN and InN can be stabilized.

The solid-state chemical reaction proposed for the GaN synthesis is the nitridation of the binary Ga oxide by again the use of Li₃N (in super-stoichiometric ratio, 50% excess as for InN), as reported in equation (2):



The results here obtained are resumed in **Table S1** while PXRD data are plotted in **Figure S5** in the Supporting Information. It was observed that the GaN hexagonal phase forms at $T \geq 600$ °C and $P \geq 2.5$ GPa. As for InN HP/HT synthesis, spurious Li-based binary and ternary oxides are always

present and a similar washing treatment was applied to successfully remove the spurious phases (**Figure S6** in the Supporting Information).

The complete double exchange reaction (see equation (2)) can be similarly obtained exploiting pristine Li_3N powders, after a HP/HT synthesis performed at 3.5 GPa, 900 °C and 3 h (**Figure 5**, upper panel). The PXRD pattern shows the presence of a pure polycrystalline GaN bulk product (**Figure 5**, bottom panel), except for few peaks with almost negligible intensity (around 33, 38 and 52°) belonging to one or more unidentified phases whose assignation is prohibitive. Raman spectroscopy data and SEM-EDX analysis confirm the obtainment of hexagonal GaN powder with the right composition of mean grain of the crystallites of about 1 μm as shown in **Figure S7** (right and left panel, respectively) in the Supporting Information.

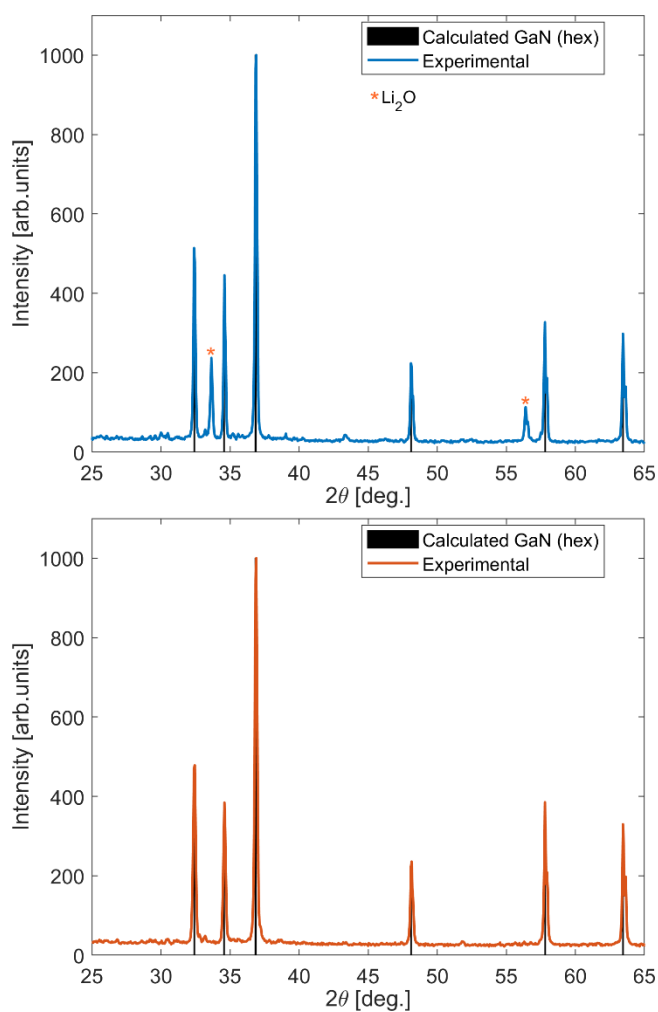


Figure 5. PXRD pattern collected for GaN after the HP/HT synthesis (upper panel) and after the subsequent washing treatment (bottom panel), obtained at 3.5 GPa and 900°C. The black lines are the calculated reflections of the GaN hexagonal phase from ICSD using POWD-12++ 23, 815(1997), while the orange “*” symbol indicate to the expected reflections of Li₂O, calculated from ICSD using POWD-12++40, 588 (1997).

Noteworthy, from these data it is clear that HP/HT technique has demonstrated to be an effective way to obtain pure bulk GaN in the same pressure regime exploited for the InN synthesis (i.e. P about 3 GPa), even though the temperature conditions required for the stabilization of the two nitrides seem to be incompatible, at least exploiting this particular solid-state reaction and these thermodynamic parameters.

4. Conclusions

In this work we reported a comprehensive study of the solid state nitridation reaction of InN from the binary oxide and Li₃N as nitrogen source, without the use of any toxic solvents or gases, following two unconventional synthesis approaches: mechanochemistry (MC) and High Pressure/High Temperature (HP/HT) synthesis.

MC reaction via high energy planetary ball milling in dry conditions pointed out that InN cannot be obtained because, at the activation threshold of the Li₃N-In₂O₃ reaction, the In-N bond is not stable, leading to an unwanted redox process with the formation of reduced metallic In and N₂. This finding suggested the application of high pressure as a viable way to guide the metastabilization of InN bond. HP/HT synthesis performed in a multi-anvil apparatus effectively allowed to perform the double exchange nitridation reaction, forming hexagonal InN polycrystalline powders and Li₂O as unique byproduct. The reaction succeeded in a wide pressure range (between 3 and 6 GPa) between 350 and 400°C. A simple washing treatment in acidic water allows to separate the InN

polycrystalline powder from the soluble Li_2O . The same method, applied for the synthesis of GaN, enables the analogous double exchange-reaction in the same HP regime but at higher temperatures.

5. Supporting Information

The Supporting Information is available free of charge at *link?*

Details on mechanochemistry of InN, additional PXRD measurements on InN synthesized by HP/HT, recap table on the GaN HP/HT syntheses and their structural characterization, SEM and Raman analysis on GaN HP/HT products, PXRD pattern of Li_3N contaminated reactant” (DOC).

6. Acknowledgment

This work has been carried out in the framework of the research project BEST4U-Technology for high Efficiency 4 terminal Bifacial Solar Cells for Utility scale (n. ARS01_00519), funded by Programma PON <<R&I>> 2014-2020 –Azione II and it has benefited from the equipment and framework of the COMP-HUB Initiative, funded by the ‘Departments of Excellence’ program of the Italian Ministry for Education, University and Research (MIUR, 2018-2022) and of the Bio-MoNTANS project, funded by Fondazione Cariparma. L.F., C.C., E.G. and D.D. sincerely thank Prof. Stefano Poli, (Department of Earth Science, University of Milan), for his technical help and advice on the high-pressure synthesis and calibration.

References

- 1 Ghosh, K.; Singisetti, U. RF performance and avalanche breakdown analysis of InN tunnel FETs. *IEEE Trans. Electron Devices* **2014**, 61(10), 3405-3410. DOI: 10.1109/TED.2014.2344914
- 2 Binari, S. C.; Doverspike, K.; Kelner, G.; Dietrich, H. B.; Wickenden, A. E. GaN FETs for microwave and high-temperature applications. *Solid-State Electron.* **1997**, 41(2), 177-180. DOI: 10.1016/S0038-1101(96)00161-X
- 3 Ren, R.; Liu, B.; Jones, E. A.; Wang, F. F.; Zhang, Z.; Costinett, D. Capacitor-clamped, three-level GaN-based DC–DC converter with dual voltage outputs for battery charger applications. *IEEE J. Emerging Sel. Top. Power Electron.* **2016**, 4(3), 841-853. DOI: 10.1109/JESTPE.2016.2586890
- 4 Davis, “Enhancement Mode GaN Delivers Impressive Performance”, Power Electronics Technology, March 2010, http://powerelectronics.com/power_semiconductors/power_mosfets/enhancement-mode-gallium-nitride-032010/index.html
- 5 <https://navitassemi.com/gan-power-ics/>
- 6 Chow, T.P.; Tyagi, R. Wide bandgap compound semiconductors for superior high-voltage power devices. In *Proceedings of the 5th International Symposium on Power Semiconductor Devices and ICs*, Monterey, CA, USA, May 18-20, 1993; 84–88. doi:10.1109/ispsd.1993.297113
- 7 Akasaki, I.; Amano, H. Breakthroughs in improving crystal quality of GaN and invention of the p–n junction blue-light-emitting diode. *Jpn. J. Appl. Phys.* **2006**, 45(12R), 9001. DOI: 10.1143/JJAP.45.9001

-
- 8 Hwang, J. I.; Hashimoto, R.; Saito, S.; Nunoue, S. Development of InGaN-based red LED grown on (0001) polar surface. *Appl. Phys. Express*, **2014**, 7(7), 071003. DOI: 10.7567/APEX.7.071003
- 9 Yeh, C. Y.; Lu, Z. W.; Froyen, S.; Zunger, A. Zinc-blende--wurtzite polytypism in semiconductors. *Phys. Rev. B*, **1992**, 46(16), 10086. DOI: 10.1103/PhysRevB.46.10086
- 10 Butcher, K.; Scott, A.; Tansley, T.L. InN, latest development and a review of the band-gap controversy. *Superlattices and Microstruct.* **2005**, 38(1), 1-37. DOI:10.1016/j.spmi.2005.03.004
- 11 Pankove, J. I. GaN: from fundamentals to applications. *Mater. Sci. Eng., B* **1999**, 61, 305-309. DOI: 10.1016/S0921-5107(98)00523-6
- 12 Schulz, H.; Thiemann, K. H. Crystal structure refinement of AlN and GaN. *Solid State Commun.* **1977**, 23(11), 815-819. DOI: 10.1016/0038-1098(77)90959-0.
- 13 Chen, P.; Chen, A.; Chua, S.; Tan, J. Growth and Optical Properties of Highly Uniform and Periodic InGaN Nanostructures. *Adv. Mater.* **2007**, 19, 1707-1710. DOI: 10.1002/adma.200602110
- 14 Wang, Y.; Zang, K.; Chua, S.; Sander, M. S.; Tripathy, S.; Fonstad, C. G. High-density arrays of InGaN nanorings, nanodots, and nanoarrows fabricated by a template-assisted approach. *Phys. Chem. B* **2006**, 110, 23, 11081–11087. DOI: 10.1021/jp060419x
- 15 Soh, C. B.; Liu, W.; Teng, J. H.; Chow, S. Y.; Ang, S. S.; Chua, S. J. Cool white III-nitride light emitting diodes based on phosphor-free indium-rich InGaN nanostructures. *Appl. Phys. Lett.* **2008**, 92(26), 261909. DOI: 10.1063/1.2952459
- 16 Oliver, R. A.; Briggs, G. A. D.; Kappers, M. J.; Humphreys, C. J.; Yasin, S.; Rice, J. H.; ... & Taylor, R. A. InGaN quantum dots grown by metalorganic vapor phase epitaxy employing a post-growth nitrogen anneal. *Appl. Phys. Lett.* **2003**, 83(4), 755-757. DOI: 10.1063/1.1595716

17 Shen, X. Q.; Tanaka, S.; Iwai, S.; Aoyagi, Y. The formation of GaN dots on $\text{Al}_x\text{Ga}_{1-x}\text{N}$ surfaces using Si in gas-source molecular beam epitaxy. *Appl. Phys. Lett.* **1998**, 72(3), 344-346.

DOI: 10.1063/1.120731

18 Lachab, M.; Nozaki, M.; Wang, J.; Ishikawa, Y.; Fareed, Q.; Wang, T.; ... Sakai, S. Selective fabrication of InGaN nanostructures by the focused ion beam/metalorganic chemical vapor deposition process. *J. Appl. Phys.* **2000**, 87(3), 1374-1378. DOI: 10.1063/1.372023

19 Yang, J. W. ; Sun, C. J. ; Chen, Q. ; Anwar, M. Z. ; Asif Khan, M. ; Nikishin, S. A. ; ... Mahajan, S. High quality GaN–InGaN heterostructures grown on (111) silicon substrates. *Appl. Phys. Lett.* **1996**, 69(23), 3566-3568. DOI: 10.1063/1.117247

20 Tourbot, G.; Bougerol, C.; Grenier, A.; Den Hertog, M.; Sam-Giao, D.; Cooper, D.; ... Daudin, B. Structural and optical properties of InGaN/GaN nanowire heterostructures grown by PAMBE. *Nanotechnol.* **2011**, 22(7), 075601. DOI: 10.1088/0957-4484/22/7/075601

21 Ting, S. M.; Ramer, J. C.; Florescu, D. I.; Merai, V. N.; Albert, B. E.; Parekh, A.; ... Armour, E. A. Morphological evolution of InGaN/GaN quantum-well heterostructures grown by metalorganic chemical vapor deposition. *J. Appl. Phys.* **2003**, 94(3), 1461-1467. DOI: 10.1063/1.1586972

22 Nakamura, S.; Senoh, M. S. M.; Mukai, T. M. T. P-GaN/N-InGaN/N-GaN double-heterostructure blue-light-emitting diodes. *Jpn. J. Appl. Phys.* **1993**, 32(1A), L8. DOI: 10.1143/JJAP.32.L8

23 Maruska, H. Pi; Tietjen, J.J. The preparation and properties of vapor-deposited single-crystal-line GaN. *App. Phys. Lett.* **1969**, 15(10), 327-329. DOI: 10.1063/1.1652845

-
- 24 Pankove, J. I. Blue anti-stokes electroluminescence in GaN. *Phys. Rev. Lett.* **1975**, 34(13), 809. DOI: 10.1103/PhysRevLett.34.809
- 25 Sasaki, T.; Zembutsu, S. Substrate-orientation dependence of GaN single-crystal films grown by metalorganic vapor-phase epitaxy. *J. Appl. Phys.* **1987**, 61(7), 2533-2540. DOI: 10.1063/1.337929
- 26 Khan, M. A.; Skogman, R. A.; Schulze, R. G.; Gershenson, M. Electrical properties and ion implantation of epitaxial GaN, grown by low pressure metalorganic chemical vapor deposition. *Appl. Phys. Lett.* **1983**, 42(5), 430-432. DOI: 10.1063/1.93953
- 27 Liu, B. L.; Lachab, M.; Jia, A.; Yoshikawaa, A.; Takahashi, K. MOCVD growth of device-quality GaN on sapphire using a three-step approach. *J. Cryst. Growth* **2002**, 234(4), 637-645. DOI: 10.1016/S0022-0248(01)01755-9
- 28 Zhang, L.; Lee, K. H.; Riko, I. M.; Huang, C. C.; Kadir, A.; Lee, K. E.; Fitzgerald, E. A. MOCVD growth of GaN on SEMI-spec 200 mm Si. *Semicond. Sci. Technol.* **2017**, 32(6), 065001. DOI: 10.1088/1361-6641/aa681c
- 29 Gotoh, H.; Suga, T.; Suzuki, H.; Kimata, M. Low temperature growth of gallium nitride. *Jpn. J. Appl. Phys.* **1981**, 20(7), L545. DOI: 10.1143/JJAP.20.L545
- 30 Yoshida, S.; Misawa, S.; Gonda, S. Improvements on the electrical and luminescent properties of reactive molecular beam epitaxially grown GaN films by using AlN-coated sapphire substrates. *Appl. Phys. Lett.* **1983**, 42(5), 427-429. DOI: 10.1063/1.93952
- 31 Tarsa, E. J.; Heying, B.; Wu, X. H.; Fini, P.; DenBaars, S. P.; Speck J. S. Homoepitaxial growth of GaN under Ga-stable and N-stable conditions by plasma-assisted molecular beam epitaxy, *J. Appl. Phys.* **1997**, 82, 5472-5479. DOI: 10.1063/1.365575

32 Moustakas, T. D.; Lei, T.; Molnar, R. J. Growth of GaN by ECR-assisted MBE. *Physica B* **1993**, *185*(1-4), 36-49. DOI: 10.1016/0921-4526(93)90213-P

33 Amano, H.; Sawaki, N.; Akasaki, I.; Toyoda, Y. Metalorganic vapor phase epitaxial growth of a high quality GaN film using an AlN buffer layer, *Appl. Phys. Lett.* **1986**, *48*, 353-355 . DOI: 10.1063/1.96549

34 Dadgar, A.; Poschenrieder, M.; Bläsing, J.; Contreras, O.; Bertram, F.; Riemann, T.; ... Krost, A. MOVPE growth of GaN on Si (1 1 1) substrates. *J. Cryst. Growth* **2003**, *248*, 556-562. DOI: 10.1016/S0022-0248(02)01894-8

35 Hiramatsu, K.; Itoh, S.; Amano, H.; Akasaki, I.; Kuwano, N.; Shiraishi, T.; Oki, K. Growth mechanism of GaN grown on sapphire with AlN buffer layer by MOVPE, *J. Cryst. Growth* **1991**, *115*(1-4), 628-633, DOI: 10.1016/0022-0248(91)90816-N

36 Imade, M.; Kishimoto, H.; Kawamura, F.; Yoshimura, M.; Kitaoka, Y.; Sasaki, T.; Mori, Y. Vapor-phase epitaxy of high-crystallinity GaN films using Ga₂O vapor and NH₃. *J. Cryst. Growth* **2010**, *312*(5), 676-679. DOI: 10.1016/j.jcrysgro.2009.12.028

37 Yoshikawa, A.; Ohshima, E.; Fukuda, T.; Tsuji, H.; Oshima, K. Crystal growth of GaN by ammonothermal method. *J. Cryst. Growth* **2004**, *260*(1-2), 67-72. DOI: 10.1016/j.jcrysgro.2003.08.031

38 Karpiński, J.; Porowski, S.; Miotkowska, S. High pressure vapor growth of GaN. *J. Cryst. Growth* **1982**, *56*(1), 77-82. DOI: 10.1016/0022-0248(82)90014-8

39 Mabuchi, A.; Iwase, Y.; Yasuda, E.; Sugiura, T.; Minoura, H. Preparation of GaN crystals by a Reaction of Ga₂O₃ with Li₃N. *J. Ceram. Soc. Jpn.* **2005**, *113*(4), 291-296. DOI: doi:10.2109/jcersj.113.291

40 Yamane, H.; Shimada, M.; Clarke, S. J.; DiSalvo F. J. Preparation of GaN Single Crystals Using a Na Flux. *Chem. Mater.* **1997**, *9*, 2, 413–416. DOI: 10.1021/cm960494s

41 Ma, H.; He, D.; Lei, L.; Wang, S.; Chen, Y.; Wang, H. GaN crystals prepared through solid-state metathesis reaction from NaGaO₂ and BN under high pressure and high temperature. *J. Alloys Compd.* **2011**, *509*(7), L124-L127. DOI: 10.1016/j.jallcom.2010.12.087

42 Lei, L.; He, D. Synthesis of GaN crystals through solid-state metathesis reaction under high pressure. *Cryst. Growth Des.* **2009**, *9*(3), 1264-1266. DOI: 10.1021/cg801017h

43 Togashi, R.; Kamoshita, T.; Adachi, H.; Murakami, H.; Kumagai, Y.; Koukitu, A. Investigation of polarity dependent InN{0001} decomposition in N₂ and H₂ ambient. *Phys. Status Solidi C* **2009**, *6*(S2 2), S372-S375. DOI: 10.1002/pssc.200880894

44 Hertrampf, J.; Becker, P.; Widenmeyer, M.; Weidenkaff, A.; Schlücker, E.; Niewa, R. Ammonothermal Crystal Growth of Indium Nitride. *Cryst. Growth Des.* **2018**, *18*, 4, 2365–2369. DOI: 10.1021/acs.cgd.7b01776

45 Chirico, P.; Hector, A.L. Solvothermal Synthesis of Gallium and Indium Nitrides Using Lithium Amide. *Z. Naturforsch., B: Chem. Sci.* **2010**, *65*(8), 1051-1057. DOI: 10.1515/znb-2010-0812

46 Dyck, J.S.; Kash, K.; Hayman, C.C. Synthesis of bulk polycrystalline indium nitride at subatmospheric pressures. *J. Mater. Res.* **1999**, *14*, 2411–2417. DOI: 10.1557/JMR.1999.0324

47 Miura, A.; Takei, T.; Kumada, N. Synthesis of wurtzite-type InN crystals by low-temperature nitridation of LiInO₂ using NaNH₂ flux. *Cryst. Growth Des.* **2012**, *12*(9), 4545-4547. DOI: 10.1021/cg3007266

48 Miura, A.; Takei, T.; Kumada, N. Low-temperature chemical synthesis of nanostructured indium nitride from indium hydroxide, *J. Ceram. Soc. Jpn.* **2020**, 128, 1, 42-45. DOI: 10.2109/jcersj2.19165

49 Gao, L.; Zhang Q.; Li, J. Preparation of Ultrafine InN Powder by the Nitridation of In₂O₃ or In(OH)₃ and its thermal stability, *J. Mater. Chem.* **2003**, 13(1), 154-158. DOI:10.1039/B208105A

50 Cumberland, R. W.; Blair, R. G.; Wallace, C. H.; Reynolds, T. K.; Kaner, R. B. Thermal control of metathesis reactions producing GaN and InN. *J. Phys. Chem. B* **2001**, 105 (47), 11922–11927 DOI: 10.1021/jp0126558

51 Choi, J.; Gillan, E.G. Low-temperature solvothermal synthesis of nanocrystalline indium nitride and Ga–In–N composites from the decomposition of metal azides, *J. Mater. Chem.* **2006**, 16, 3774-3784, DOI: 10.1039/B608204A

52 Real, C.; Roldan, M. A.; Alcala, M. D.; Ortega, A. Synthesis of nanocrystalline chromium nitride powder by mechanical processing. *J. Am. Ceram. Soc.* **2007**, 90(10), 3085-3090. DOI: 10.1111/j.1551-2916.2007.01898.x

53 Xu, X.; Nishimura, T.; Hirosaki, N.; Xie, R.-J.; Zhu, Y.; Yamamoto, Y.; Tanaka, H. New Strategies for Preparing NanoSized Silicon Nitride Ceramics. *J. Am. Ceram. Soc.* **2005**, 88, 934-937. DOI: 10.1111/j.1551-2916.2005.00187.x

54 Sun, Y.; Yao, B.; He, Q.; Su, F.; Wang, H. Z. Synthesis and formation mechanism of cubic ZrN nanopowders by mechanochemical reaction of ZrCl₄ and Li₃N. *J. Alloys Compd.* **2009**, 479(1-2), 599-602. DOI: 10.1016/j.jallcom.2008.12.149

55 Kano, J.; Kobayashi, E.; Tongamp, W.; Saito, F. Preparation of GaN powder by mechanochemical reaction between Ga₂O₃ and Li₃N. *J. Alloys Comp.* **2008**, 464 (1-2), 337-339.

DOI: 10.1016/j.jallcom.2007.09.120

56 Sun, J. F.; Wang, M. Z.; Zhao, Y. C.; Li, X. P.; Liang, B. Y. Synthesis of titanium nitride powders by reactive ball milling of titanium and urea. *J. Alloys Comp.* **2009**, 482(1-2), L29-L31.

DOI: 10.1016/j.jallcom.2009.04.043

57 Chen, Y.; Halstead, T.; Williams, J. S. Influence of milling temperature and atmosphere on the synthesis of iron nitrides by ball milling. *Mater. Sci. Eng., A* **1996**, 206(1), 24-29. DOI:

10.1016/0921-5093(95)09977-8

58 Shatskiy, A.; Borzdov, Y. M.; Yamazaki, D.; Litasov, K. D.; Katsura, T.; Palyanov, Y. N. Aluminum Nitride Crystal Growth from an Al–N System at 6.0 GPa and 1800° C. *Cryst. Growth Des.* **2010**, 10(6), 2563-2570. DOI: 10.1021/cg901519s

59 McMillan, P. F. New materials from high-pressure experiments. *Nat. Mater.* **2002**, 1(1) 19–25 (2002). DOI: 10.1038/nmat716

60 Leinenweber, K.; O'keeffe, M.; Somayazulu, M.; Hubert, H.; McMillan, P. F.; Wolf, G. H. Synthesis and structure refinement of the spinel, γ -Ge₃N₄. *Chem.–Eur. J.* **1999**, 5(10), 3076-3078.

DOI: 10.1002/(SICI)1521-3765(19991001)5:10<3076::AID-CHEM3076>3.0.CO;2-D

61 Solozhenko, V. L.; Dub, S. N.; Novikov, N. V. Mechanical properties of cubic BC₂N, a new superhard phase. *Diamond Relat. Mater.* **2001**, 10(12), 2228-2231. DOI: 10.1016/S0925-9635(01)00513-1.

62 Solozhenko, V.L.; Bushlya, V. Mechanical properties of superhard boron subnitride B₁₃N₂. *J. Superhard Mater.* **2017**, 39, 422–426. DOI: 10.3103/S1063457617060065

63 Soignard, E.; McMillan, P. F.; Chaplin, T. D.; Farag, S. M.; Bull, C. L.; Somayazulu, M. S.; Leinenweber, K. High-pressure synthesis and study of low-compressibility molybdenum nitride (MoN and MoN_{1-x}) phases. *Phys. Rev. B* **2003**, 68(13), 132101. DOI: 10.1103/PhysRevB.68.132101

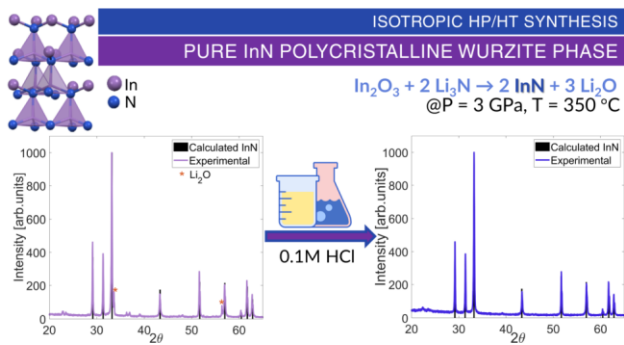
64 Zerr, A.; Miehe, G.; Serghiou, G. et al. Synthesis of cubic silicon nitride. *Nat.* **1999**, 400(6742), 340–342. DOI: 10.1038/22493

65 Gregoryanz, E.; Sanloup, C.; Somayazulu, M. et al. Synthesis and characterization of a binary noble metal nitride. *Nat. Mater.* **2004**, 3(5), 294–297. DOI: 10.1038/nmat1115

66 Peiris, S. M.; Russell, T. P. Photolysis of compressed sodium azide (NaN₃) as a synthetic pathway to nitrogen materials. *J. Phys. Chem. A* **2003**, 107(6), 944–947. DOI: 10.1021/jp025963u

67 Grzegory, I.; Jun, J.; Krukowski, S.; Perlin, P.; Porowski, S. InN thermodynamics and crystal growth at high pressure of N₂. *Jpn. J. Appl. Phys.* **1993**, 32(S1), 343. DOI: 10.7567/JJAPS.32S1.343

68 Inushima, T.; Shiraishi, T.; Davydov, V. Y. Phonon structure of InN grown by atomic layer epitaxy. *Solid State Commun.* **1999**, 110(9), 491-495. DOI: 10.1016/S0038-1098(99)00108-8



For Table of Contents Only

Synopsis

Bulk indium nitride was successfully grown by means of a simple solid-state chemical reaction carried out under hydrostatic high pressure/high temperature conditions in a multi-anvil apparatus, starting from the binary oxide and Li_3N as nitridation agent, not involving gases or solvents during the process. Simple washing treatment in acidic water allows to remove the unique byproduct (Li_2O) from the sample, obtaining pure polycrystalline indium nitride hexagonal phase.